International Journal on Recent Researches In Science, Engineering & Technology
(Division of Computer Science and Engineering)
A Journal Established in early 2000 as National journal and upgraded to International journal in 2013 and is in existence for the last 10 years. It is run by Retired Professors from NIT, Trichy. It is an absolutely free (No processing charges, No publishing charges etc) Journal Indexed in JIR, DIIF and SJIF.
Research Paper
Available online at: www.jrrset.com

ISSN (Print) : 2347-6729
ISSN (Online) : 2348-3105
Volume 4, Issue 12, December 2016.
JIR IF : 2.54
DIIF IF : 1.46
SJIF IF : 1.329

ACCURATE SEGMENTATION OF NON-IDEAL IRIS IMAGES

Ratheesh Kumar S,Prajeesh R, Sony Sethukumar

Department of Electronics and Communication, Sri VellappallyNatesan College of Engineering, Pallickal P.O, Mavelikkara, Alappuzha 690503.

Abstract

Iris biometric is one of the most reliable biometric with respect to performance. The accuracy of iris recognition depends on the accuracy of iris segmentation. But the process of segmenting iris from non-ideal iris images is a challenging task. In this paper, a segmentation methodology that aims at compensating various nonidealities contained in iris images during segmentation is proposed. The nonideal iris images are those images affected with specular reflection, blur, lighting variation, occlusion and off-angle images. Our algorithm involves two phases. In the first phase, the non-ideal factors are compensated. In the second phase, segmentation of iris is performed using ellipse fitting. Since the nonidealities are compensated, the improvement in the accuracy of segmentation is guaranteed. We demonstrate the robustness of our segmentation methodology by evaluating the data set, namely, the Chinese Academy of Sciences iris data version3 interval subdirectory.

Keywords: Iris Segmentation, Specular Reflection, blur, occlusion, off-angle, ellipse fitting

1. Introduction

In recent years, iris recognition has gathered a great importance due to its reliability. Current iris recognition algorithms that have potential for high recognition performance require highly constrained subject presentation. But in practical situations, the subject presentation (capture of iris images) cannot be constrained and so the quality of the captured data may be degraded. These factors, such as specular reflection, lighting variation, blur, off-angle, and occlusion can negatively impact segmentation performance.

Clasically, pupil and iris regions have been localized using efficient integrodifferential operator as defined by Daugman[7]. This operator remains in use today for a majority of commercial systems. Wildes[23] introduced pupil and iris localization by use of edge detection, which is followed by circular Hough transform. A number of recent approaches, based on variants of the former methodology that utilize the Hough Transform, have been developed ([5], [22]). Some algorithms has employed morphological operators and ellipse fitting to cope with the noncircular shape of iris. The

limitation concerning these algorithms is that they were developed for ideal data. This may result in significant degradation of performance when the algorithms are applied to nonideal imagery.

There have been some work focusing on non-ideal iris specifically off-angle [19].They mostly focus on bringing off-angle iris images into frontal view to involve iris segmentation algorithms defined for frontal view ideal irises, rather than dealing with the segmentation aspects related to this paper. Proenca and Alexandre[15] identify a more noise-tolerant feature set, consisting of pixel location and intensity, which is then uses to construct an edge map followed by circular Hough transform for localization. They demonstrate good results when evaluating the UBIRIS data set. One disadvantage with this approach is that inexact localization can result from off-angle images because of the circular fit.

Some authors([24]) claim that their optimal partitioning-based algorithm is robust to poor illumination, blur, occlusion. The method of segmentation based on graph cuts[16] is an unique approach. But this technique is very complex. Some papers provides methods for the estimation of occlusions and also to eliminate the presence of specular reflections. The most recent trend is to use active contours. The author of [17] has used a Fourier based trigonometry to approximate the iris boundary from a set of Fourier coefficients. The difficulty with this approach is that it is difficult to determine the required order of Fourier Expansion. Actually most of the authors have used Hough transform in one way or the other. Hough transform is very efficient while dealing with ideal iris images. But the efficiency is reduced in case of non-ideal iris images.

In this paper, we propose a methodology for automatic segmentation of iris images that sequentially compensates non-ideal factors present in poor quality iris images. The fact that quality metrics can individually be estimated laid a foundation for this paper. This paper describes a sequence of procedures and steps that are intended to compensate detected nonidealities in iris images to successfully segment nonideal iris images. The following compensation steps are applied. We first detect and eliminate specular reflections through the application of hard thresholding and partial differential equation based inpainting. Then we localize the pupil by invoking diverse information available in the image involving pupil location, intensity and shape. We further propose a technique to eliminate occlusions resulting from the overlap of long eyelashes with the area of the pupil. Both the pupil and the iris are segmented by fitting a rotated ellipse, which is an ellipse parameterized by the parameters of the main axes, center point, and the angle of rotation. Simultaneously with the iris boundary we estimate the occlusion mask by applying an edge detector and slightly smearing the mask to ensure connected edges.

The rest of this paper is organized as follows. Section II describes our processing steps for non-ideal images and segmentation methodology for pupil and iris localization. Section III illustrates the performance of our segmentation algorithm. Finally conclusion is presented in section IV.

2. Proposed Algorithm

Our iris segmentation algorithm includes the following steps. A) preprocessing B) pupil segmenation C) iris segmentation D) occlusion estimation and E) unwrapping.

A. Preprocessing

1) Inpainting of Specular reflections: Specular reflections appear as white bright spots in the image. If they are not removed, they can degrade the performance of an intensity and gradient-based segmentation algorithm.

Let A(n1, n2) be an image intensity at a location (n1, n2). The parametersγ_1, γ_2, τ (maximum pupil intensity value)have to be preset and their values depends on the type of sensors used to get the image. The thresholding function γ (n1, n2) is given as:

$$\gamma(n1,n1) = \begin{cases} \gamma_1 & \text{Pixel located outside pupil area.} \\ \gamma_2 & \text{Pixel located inside the pupil area determined by } \tau. \end{cases} \quad (1)$$

The intensity value of the pixel (n1, n2) is considered as a specular reflection if the intensity value A(n1, n2) ≥ γ (n1, n2).

The parameters can easily be estimated from a small set of sample iris images when the capture device or the environmental setup changes. The set of parameters that we have used to demonstrate the performance of this algorithm is suitable for a number of iris capture devices operating in a near-IR range. The complete inpainting procedure includes the following steps:

1) A potential pupil area (mask p1) is identified using the threshold τ. An enlarged mask p2 is obtained after closing unfilled regions.
2) Potential regions containing specular reflections are selected, i.e., masks are selected using the thresholding procedure(1)
3) Mask s is dilated to include all the possible affected regions.
4) The intersection of mask p2 and mask s is obtained as mask p3.
5) The pixel is considered to be affected with specular reflection if it satisfies the following condition:
   A) The value of the pixel p1(p,q) is 0.
   B) The value of the pixel p2(p,q) is 1.
   C) The value of the pixel p3(p,q) is 1.
6) If the pixel is identified to be affected with specular reflection, then it has to be inpainted(replace with normal pixel).
7) A PDE based inpaintingprocedure[2] is used to replace the affected pixel with the normal pixel.

The results are clearly shown in Fig.1

2) Denoising:We have used a 2-D adaptive Wiener filter to remove the effect of noise (if present). The value of mean and variance are locally estimated first for each pixel (n1, n2) in the original

image. Then the image is denoised. A 5×5 neighborhood is used. The effect of noise removal is particularly noticeable in low-resolution images.

B. Pupil Segmentation

1) Contrast Enhancement:This step is required to guarantee the clarity of boundary between the pupil and the iris. It ensures correct pupil segmentation.

2) Smoothing:Noise and other strong disturbances caused by the eyelashes and near-pupil sphincter muscle are eliminated by performing the smoothing step. We used a median filter with 5×5 neighborhood to remove the misleading edges inside the iris area. As the pupil segmentation procedure is intensity and gradient based, the smoothing of the image is important for the images with low contrast or with a noisy pupil area.

3) Pupil Localisation: We have made two assumptions to localize the pupil.

1) Pupil area has the smallest intensity values.

2) Shape of pupil is described by a circle or ellipse

We have used two steps to locate the pupil.

1. Pupil candidates are selected based on a circular shape by Hough Transform.
2. The optimal candidate is selected based on the value w_i for each candidate i.

$$w_i = = \frac{I_i}{1+3d_i^2} \text{ where} \quad (2)$$

$d_i$is the distance between candidate and image center

I_i is the intensity value of the candidate at location i.

The optimal candidate is chosen to be the candidate with largest value w_i. Once the optimal candidate is selected, the pupil can be roughly segmented using the similarity of intensity values. Fig. 2 is an illustration of this process.

4) Rough Segmentation of the pupil: A 5×5 neighborhood around the optimal candidate is used to identify the initial minimum and maximum intensities used for searching the pupil area. This intensity range is defined based on the rough estimation of the pupil shape and the gradient information along

the region boundary. The pupil area is assumed to be relatively well described by a circular shape and has a clear boundary. The summary of evaluation criteria is:

1) The size of the selected area should be larger than a threshold. We use 100.

2) The average gradient value along the boundary has to be maximum.

After the rough evaluation, we perform a few more processing steps to compensate for eyelash occlusion and specular reflections on the papillary boundary.

5) Refinement of the Pupil Boundary: Eyelashes can introduce “spike”-like shapes along the boundary. The center of mass for the rough segmentation region is used as an approximation to the pupil center. The boundary is scanned and spikes are detected (using the distance from the boundary points to the center or by using angular information). Detected spikes are removed by using a large circle of radius that is equal to twice the distance from the cutting point to the center. Fig. 3 illustrates this procedure.

Strong specular reflections along the pupil boundary or light colored eyelashes may cause the rough pupil boundary to become concave which may degrade. We calculate the convex hull with respect to the pupil boundary to reduce this problem. An illustration of this process is provided in the Fig. 4.

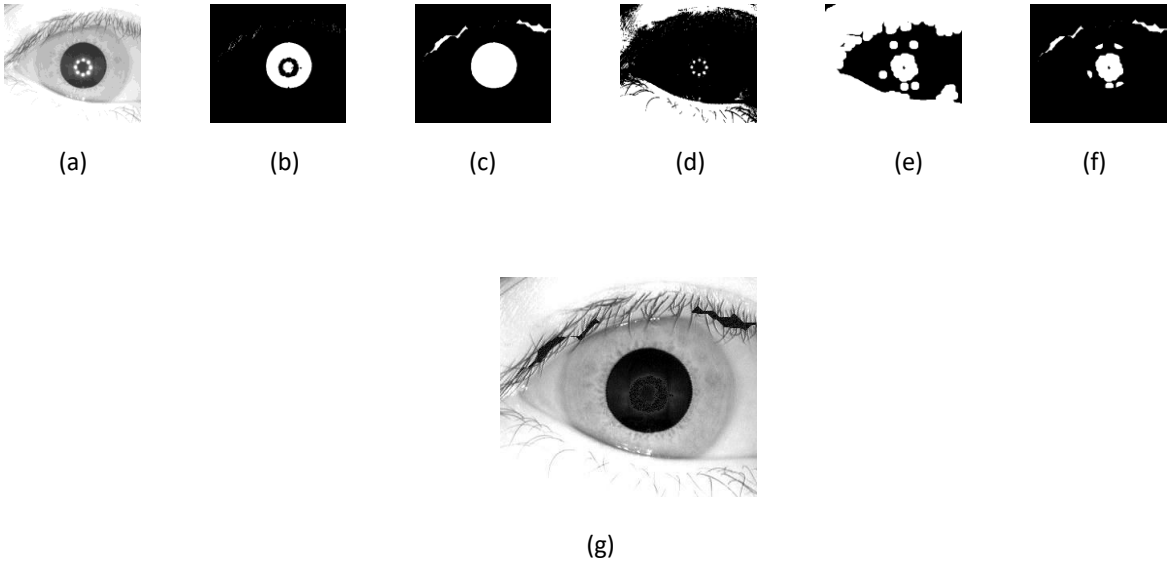

(a) (b) (c) (d) (e) (f)

(g)

Fig. 1. (a) Iris Image (b)Mask p1 (c) Mask p2 (d) Mask s (e) Mask s dilated (f) Mask p3 (g) Inpainted Image

Fig. 2. Six pupil candidates are selected based on a circular shape of bright regions. Then, the intensity information is used to select the optimal candidate with the largest intensity value.

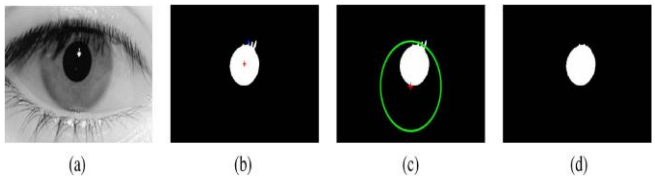

Fig. 3. "Spike" removal. (a) Original Image (b) Estimated pupil boundary (c) Removing the "spike" (d) Refined boundary after the "spike" removal.

Fig. 4. "Spike" removal. (a) Original Image (b) Initial concave pupil mask (c) convex hull result (d) result of ellipse-fitting using an unaffected pupil boundary.

6) Ellipse Fitting:We have used a rotated ellipse model to describe the pupil boundary. Mathematically, a rotated ellipse is described as

$$\frac{((x-x_0)cos\varphi+(y-y_0)sin\varphi)^2}{a^2}+\frac{((x-x_0)sin\varphi+(y-y_0)cos\varphi)^2}{b^2}=1 \quad (3)$$

Where (x_o,y_o) is the center of the pupil, and φ is the angle of rotation. The boundary (partial) is selected using only those points that lie outside the specular reflection mask generated during the inpainting procedure. The top and bottom parts of the boundary should be avoided to overcome occlusions. The conditions to be considered while selecting the partial boundary are:

1) The part should be outside of the specular reflection mask.

2) It should have a clear edge (high gradient value).

3) It should be continuous.

The goodness of the pupil boundary estimation is verified using two criteria.

1) The error between the pupil mask and the ellipse fitted into the boundary should be small.

2) If only a small part of the pupil remains unoccluded, sections of the pupil boundary have to be well separated.

Fig. 5 illustrates the ellipse fitting procedure.

C. Iris Segmentation

We assume that the shapes of the iris and the pupil are similar and apply (2) to segment the iris region. Other assumptions that reduce the computational cost can be made. They include using the

same angle φ and same parameters a and b. These assumptions are particularly useful when the iris is heavily occluded or it is strongly rotated.

1) Image Translation and Inpainting: To ensure that the search of the limbic boundary is performed over a broad range of parameters describing the ellipse, the image of an iris is translated such that the center of the pupil is aligned with the center of the image. The blank area formed due to the image shift is inpainted to avoid introduction of new edges. An example of an image containing a partial iris is shown in Fig. 6.

2) Directional Edge Detector: We use a method similar to Daugman's edge detector based on integrodifferentialoperator[3]. Define a space of rotated ellipse(3) where the center of the iris is limited to the neighborhood of the center of the pupil. The problem of finding the best fit is reduced to the following optimization problem:

$$\text{Max}\left[\frac{1}{L(r,x_{io},y_{io})}\int_{B(r,x_{io},y_{io})} F\left(\nabla(I(x,y))\right) ds\right] \quad (4)$$

Where $B(r,x_{io},y_{io})$ is the partial boundary of the ellipse and $L(r,x_{io},y_{io})$ is the length of $B(r,x_{io},y_{io})$, and $F(\nabla(I(x,y)))$ is a function of the image gradient. The function $L(r,x_{io},y_{io})$ is the normalization given by

$$L(r,x_{io},y_{io}) = \int_{B(r,x_{io},y_{io})} 1\, ds \quad (5)$$

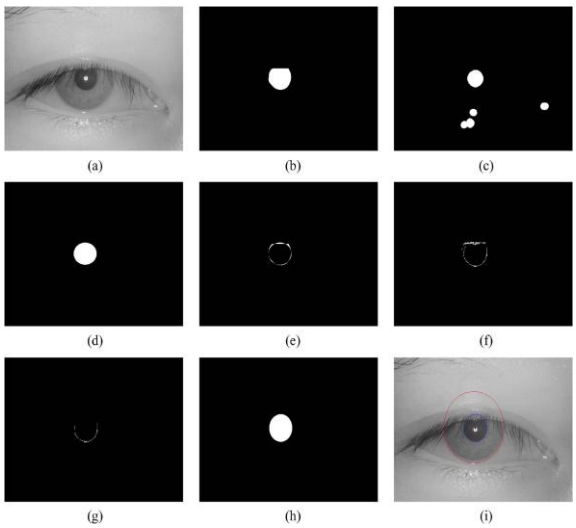

Fig. 5.Ellipse Fitting. (a) Original Image (b) Refined pupil mask (c) Specular reflection mask (d) ellipse fitting taking into account specular reflections (e) Error(the Exclusive-or between ellipse fitting

with the original refined pupil mask) (f)edges detected near the refined pupil boundary (g) selected partial boundary (h) new ellipse fitting result using the partial boundary (i) final segmentation result

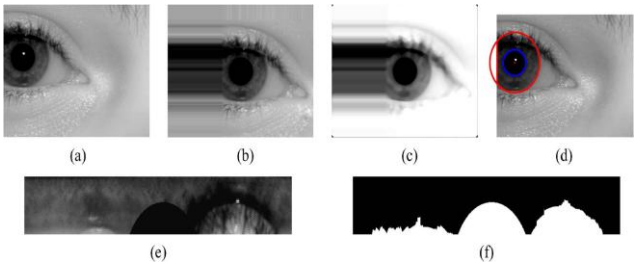

Fig. 6 Image translation procedure (a)original image (b) image after translation and inpainting (c) enhanced image (d) segmented iris (e) unwrapped template (f)unwrapped template mask.

The function F($\nabla(I(x,y))$) can be evaluated on an unwrapped image as shown in Fig. 7. The transformation of an elliptical system into a circular system is given by

$$(x - x_o)cos\varphi + (y - y_o)sin\varphi = \text{ar cos}\theta' \quad (6)$$

$$-(x - x_o)sin\varphi + (y - y_o)cos\varphi = \text{br sin}\theta'$$

Where θ' = (θ- φ') and φ' = arctan((a/b) tan φ). The angle φ' is used to map the three o'clock point on the ellipse in the three o'clock point on the circle assuming θ = 0. Then the normal direction to the ellipse described by (3) will correspond to the vertical direction in the unwrapped image displayed in the polar coordinate system(r, θ), i.e.,

$$\text{F}([U_o, U_r]) = \begin{cases} U_r U_r > 0 \\ 0\ elsewhere \end{cases} \quad (7)$$

Where $U_o and\ U_r$ are the gradients of image U in θ and r directions respectively. The polar representation of the iris is further used to efficiently find the boundary of the iris B(r, x_{io}, y_{io}).

3) Contrast Compensation: Besides heavy occlusion, the uneven illumination of the iris may cause an "offset" during the estimation of the iris boundary since all points on the boundary are treated equally. The gradient difference along the iris boundary, resulting from an uneven illumination, cause the left edge of the iris to be more pronounced compared with the right edge. This problem can be solved by normalizing the gradients before fitting an ellipse. Since the pupil is segmented at this stage the iris images can be unwrapped with respect to the pupil center. The right and left portions of the

unwrapped iris are then considered separately. The iris boundaries are detected separately too. The summation of the gradient values along the boundary on each side is used to calculate the weights to balance the segmentation. To achieve the correct segmentation of the iris, we scale the right and left boundaries of the iris by estimated weights that balance the contribution into the complete ellipse fitted into the iris. The details of the contrast balancing procedure are clearly shown in fig. 8.

D. Occlusion Estimation:

We implement an occlusion estimation method based on edge detection. To detect horizontaledges, we implement a few steps. We first convolve a horizontal sobel mask with the iris image. Let b_y be the result of the convolution. We compare b_y^2 with the square of the sensitivity threshold β at every pixel location (n1, n2). If $b_y(n1,n2)^2 > \beta^2$ and if it is a local maximum, then a horizontal edge point is detected at position (n1, n2). The process of estimating occlusions is further illustrated in Fig. 9.

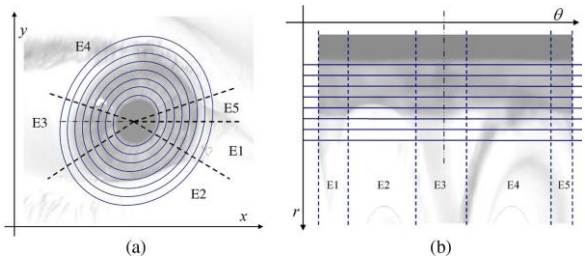

Fig. 7. (a) Original image showing an off-angle iris. (b)Same iris transformed into the circular coordinate system and unwrapped. The regions E1, E3, and E5 contain the true boundary between the iris and the scelera.

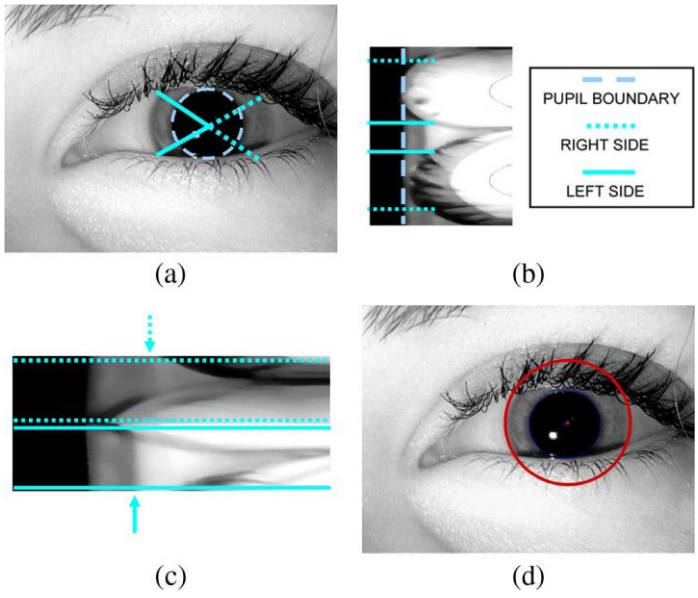

Fig. 8. Contrast balancing procedure. (a) original image with results of pupil segmentation imposed onto the image (b) unwrapped image (c) iris boundaries are separately detected(d) result of the final iris detection with different contrast compensation weights added on both sides.

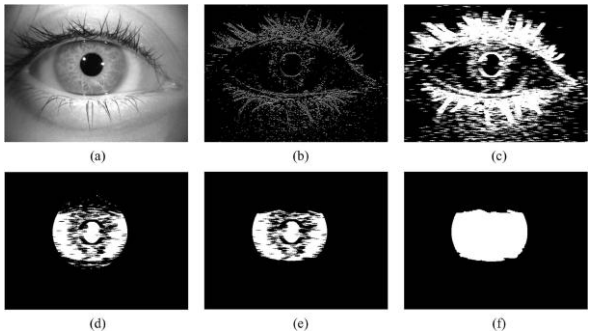

Fig. 9. Evolution of the occlusion mask.(a) Original Image (b) result of the initial edge detection (c)edge information after smearing(d) result of combination of the mask and outcome of iris segmentation (e) area selected based on connectivity information. (f) Final result

E. Unwrapping:

To unwrap the iris, we use a technique similar to Camus and Wildes technique [1]. Both the iris and the pupil are described by ellipses. The boundaries are sampled and mapped into circles. The ellipse describing the pupil boundary is given by

$$x_p(\theta) = a_p\cos(\theta-\varphi'_p)\cos\varphi_p - b_p\sin(\theta-\varphi'_p)\sin\varphi_p + x_{po}$$

$$y_p(\theta) = a_p\cos(\theta-\varphi'_p)\sin\varphi_p + b_p\sin(\theta-\varphi'_p)\cos\varphi_p + y_{po}$$

Where $(x_{po}, y_{po}, a_p, b_p, \varphi_p)$ are the parameters of the ellipse. The iris boundary is described by the ellipse with the parameters

$$x_i(\theta) = a_i\cos(\theta-\varphi'_i)\cos\varphi_i - b_i\sin(\theta-\varphi'_i)\sin\varphi_i + x_{io}$$

$$y_i(\theta) = a_i\cos(\theta-\varphi'_i)\sin\varphi_i + b_i\sin(\theta-\varphi'_i)\cos\varphi_i + y_{io}$$

The mapping of the point (x', y') into (θ, r) point in the pseudopolar coordinate system is described by

$$x'(\theta, r) = (1 - r)x_p(\theta) + rx_i(\theta)$$

$$y'(\theta, r) = (1 - r)y_p(\theta) + ry_i(\theta)$$

Where $0 < r \leq 1$, (x_p, y_p) is a sample point on the pupil boundary, and (x_i, y_i) is a sample point on the iris boundary. Finally the pixel intensity is interpolated using a cubic interpolation method to generate the unwrapped iris.

3.Performance Evaluation

To verify the performance of the proposed segmentation algorithm, we perform visual evaluation. The criteria used for visual evaluation is shown in Fig. 10. We select two criteria as a measure of visual evalution: the maximum offset of the pupil boundary ε_p and the maximum offset of the iris boundary ε_i. The two offsets will be compared with the minimum distance between the iris boundary and the pupil. i.e., min_d. All results are placed in four categories.

Good: $\varepsilon_p / min_d < 5\%$ and ε_i / min_d <10%. There is no clear boundary offset.

Fair: (5%$\leq \varepsilon_p/min_d < 10\%$ and $\varepsilon_i / min_d < 20\%$.) or ($\varepsilon_p/min_d < 10\%$ and 10%$\leq \varepsilon_i/min_d$ <20%).

Poor: (10%$\leq \varepsilon_p/min_d < 20\%$ and $\varepsilon_i/min_d < 35\%$) or ($\varepsilon_p/min_d < 20\%$ and 20%$\leq \varepsilon_i/min_d$ <35%).

Bad: Everything else.

The examples of good, fair, poor and bad segmentations are shown in Fig. 11.

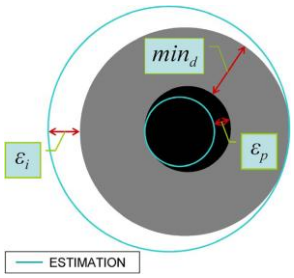

Fig.10. Criteria used for visual evaluation of the proposed algorithm.

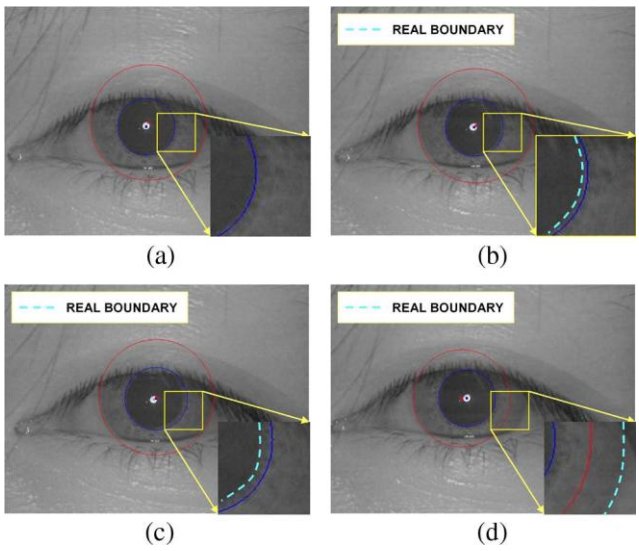

Fig. 11. Examples of (a)good (b)fair (c)poor (d)bad segmentations

Table 1 contains the results of manual evaluation of the segmentation performance of the proposed algorithm.

TABLE I
Results of manual performance evaluation.

CASIA 3INT dataset of iris images	Good	95.31%	Correct=Good+Fair 98.06%
	Fair	2.75%	
	Poor	1.49%	Incorrect=Poor+Bad 1.94%
	Bad	0.45%	

4. Conclusion and Future work

A methodology for robust iris segmentation designed specifically for nonideal irises has been proposed. Processing steps were done to deal with non-idealities like specular reflections. An ellipse-based model is used to model the boundaries of iris which can effectively handle nonfrontal iris images also. The occlusion is also detected. We evaluated the performance of our algorithm by using the dataset namely CASIA 3INT iris dataset and we achieved a very high rate of accuracy. This algorithm can guarantee an excellent rate of accuracy in iris segmentation and can be used in iris recognition algorithms to improve their accuracy.

In the future, we intend to increase the speed of our algorithm. The use of active contours as a tool for more precise segmentation is also a possible extension to our work.

References

[1] A.R Kiruthiga (Mar 2017), “Smoothening if iris images and pupil segmentation using fractional derivative and wavelet transform”
[2] Abhishek Gangwar(Aug 2016), “ A fast and robust iris segmentation framework for non-ideal iris images”

[3] Camus T. A and R. Wildes, (Aug 2002), "Reliable and Fast Eye Finding in Close-Up Images," in Proc. 16th Int. Conf. Pattern Recog., vol. 1, pp.389-394.

[4] B K Meenakshi, (Dec 2014),"Segmentation of iris images which are affected by light illuminations"

[5] Chan. T, Shen. J, (jan 2003), "Variational PDE models in image processing", Am. Math. Soc., vol 50, no. 1, pp.14-26

[6] Daugman .J, (1993) "High Confidence Visual Recognition of Persons by a test of Statistical Independence," IEEE Trans. Pattern Anal. Mach. Intell., vol. 15, no. 11, pp. 1148-1161

[7] Daugman. J, (Oct 2007), "New Methods in Iris Recognition," IEEETrans.Syst., Man, Cybern. B. Cybern., vol 37, no. 5, pp. 1167-1175.

[8] Jing-Hui Li, Jian-Hua Wu and De-Xuan Zou , (2009), "New Algorithm of Iris Localizaion", IEEE world congress on Computer Science and Information Technology.

[9] JinyuZuo, Nathan D. Kalka, and Natalia A. Schmid, (2006), "A Roust Segmentation Procedure for Unconstrained Subject Presentaion", IEEE

[10]Joke A Badejo,(2016), A robust preprocessing algorithm for iris segmentation from low contrast eye images.

[11]Kong. K, Zhang. D, (Sep 2003) "Detecting eyelash and reflection for accurate iris segmentation," Int. J. Pattern Recog. Artif.Intell. Vol. 17 pp 1025-1034

[12]Liu. X, Bowyer K. W, (2005), "experiments with an improved iris segmentation algorithm," in Proc 4th IEEE Workshop Autom pp.118-123

[13]Mohammed A.M Abdullah, (2017), Robust iris segmentation method Based on a new active contour force with a noncircular normalization.

[14]Nguyen Van Huan and Hakil Kim, (2008), "A novel Circle Detection method for Iris Segmentation", IEEE congress on image and signal processing.

[15]Proenca.H and Alexandre.L, (Apr 2006), "Iris Segmentation Methodology for Non-cooperative Recognition," Proc. Inst. Elect. Eng.-Vision, image signal Process., vol. 153, no. 2, pp. 199-205.

[16]Pundik. S. J, Woodard. D. L, and Birchfield. S. T, (Jun 2008), "Non-Ideal Iris Segmentation using Graph Cuts, " in Proc. IEEE Comput. Soc. Conf. CVPR Workshops, pp. 1-6

[17]Puhan. N. B, Sudha. N, and Jiang. X, (Dec 2007), "Robust Eyeball Segmentation in Noisy Iris Images using Fourier Spectral Density," in Proc. 6th Int. Conf. Inf., Commun. Signal Process., pp. 1-6.

[18]SasanHarifi (2015),"efficient iris segmentation based on converting iris images to high dynamic range images".

[19]Schuckers. S, Abayankar. A, (2005) ,"Off angle iris recognition using bi-orthogonal wavelet network system", in Proc 4th IEEE Workshop pp . 239-244

[20]Sheikh Akbari,(2015),"Iris segmentation using a non decimated wavelet transform.

[21]Sung. E, Chen. X,(Dec 2002), "Towards non-cooperative iris recognition systems," in Proc. Vol2. Pp. 990-995

[22]Tian .Q, Pan. Q, Cheng. Y, and Gao, (Aug 2004) Q, "Fast Algorithm and Application of Hough Transform in Iris Segmentation." In Proc. 3rd Int. Conf. Mach. Learn. Cybern., Shanghai, China, vol. 7, pp. 3977-3980.

[23]Wildes. R. P,"Irisrecognition:an emerging biometric technology", Proc IEEE, vol.85, no.9,pp 1348-1363 ,sep 1997

[24]Zaim.A, Quweider. M, Scargle. J, Iglesias. J, and R. Tang, (Aug 2006), "A robust and accurate segmentation of iris images using optimal partitioning," in Proc. Int. Conf. Pattern Recog., pp. 479-485

[25]Hung. J,"Noise removal and inpainting model for iris images," in Proc.Int. Conf. Image Process., Oct.2004. vol.2 pp.869-872G. Shafer.

[26]G. Shafer, *AMathematical Theory of Evidence*. Princeton, NJ: Princeton Univ. Press, 1976.

[27]Center for Biometric Authentication and Testing, Institute of Automation,

Chinese Academy of Sciences, China, *CASIA Iris Database (ver. 3.0)*.[Online]. Available: http://www.cbsr.ia.ac.cn/IrisDataBase.htm